The breakdown of Fermi liquid theory in the Hubbard model: II

1993 J. Phys.: Condens. Matter 5 161

(http://iopscience.iop.org/0953-8984/5/2/004)

J. Phys.: Condens. Matter 5 (1993) 161–170. Printed in the UK

The breakdown of Fermi liquid theory in the Hubbard model: II

D M Edwards
Department of Mathematics, Imperial College, London SW7 2BZ, UK

Received 9 September 1992

Abstract. An exact diagrammatic analysis of the electron self-energy in the Hubbard and related models is given within the local approximation. Contact is made with recent work for dimension $d = \infty$ where the local approximation becomes exact. It is shown that the approximate method of paper I of the series may be fitted into the new framework and yields sensible results for the Anderson impurity model. This lends weight to the prediction of I that for paramagnetic solutions of the Hubbard model Fermi liquid behaviour breaks down in a whole region of the $T = 0$ phase diagram, not just for a half-filled band where the Mott transition occurs.

1. Introduction

In the first paper of this series [1], referred to here as I, a new approach to the Hubbard model [2] was introduced. The Hubbard alloy analogy approximation [2] was modified so as to recover Fermi liquid behaviour for small U/W, where U is the on-site interaction between electrons and $2W$ is the bandwidth. It was found that, for low-electron density, Fermi liquid behaviour, characterized by a normal Fermi surface marked by a Migdal discontinuity in the Bloch-state occupation number $\langle n_{k} \rangle$, persisted for all U/W. However, nearer half filling Fermi liquid behaviour was found to break down at larger U/W. The calculation showed a phase transition at $T = 0$ between a normal Fermi liquid and a non-Fermi liquid along a curve in the δ versus U/W phase diagram, where $\delta = 1 - 2n$ and n is the number of electrons per atom per spin. The method used to obtain these rather striking results of I is exact in certain limits, within the local approximation discussed below, but of uncertain accuracy in between. In this paper we formulate a theory which is formally exact within the local approximation. It is shown that the approximate method of I falls within the general framework of this theory which lends more weight to the results of I. It is now known [3, 4] that the local approximation is exact for $d = \infty$, where d is the number of spatial dimensions, and in this limit the present theory provides a new derivation of a recently derived calculational scheme which in principle is exact [5–7].

2. Exact diagrammatic formulation of the self-energy within the local approximation

To be specific we shall consider the Hubbard model [2] with Hamiltonian

$$\mathcal{H} = \sum_{ij\sigma} t_{ij} c_{i\sigma}^{\dagger} c_{j\sigma} + U \sum_{i} n_{i\uparrow} n_{i\downarrow} \tag{2.1}$$

0953-8984/93/020161+10$07.50

in the usual notation. We shall consider proper self-energy diagrams at $T = 0$ although the generalization to finite T is immediate. These diagrams have the same structure for any other model with electron interaction restricted to the on-site form of the second term in $\mathcal{H}$. Only the unperturbed propagator G^0_{ij} is different for different models. The one-electron term, the first in $\mathcal{H}$, may include hopping between orbitals associated with more than one band so that the class of Hamiltonians we may consider includes the periodic Anderson model and the d–p model of CuO_2 planes as well as the Anderson impurity model.

We recall that the Hubbard alloy analogy approximation [2] consists in calculating the self-energy for electrons of spin σ using the one-electron Hamiltonian obtained by the replacement $n_{i\sigma}n_{i-\sigma} \rightarrow n_{i\sigma}\langle n_{i-\sigma}\rangle$ in equation (2.1). The $\langle n_{i-\sigma}\rangle$ take values 0 or 1 and a configuration average over the positions of the 'frozen' $-\sigma$ spin is carried out using the coherent potential approximation (CPA). This is the best single-site, or local, approximation for the alloy self-energy and corresponds to an electron in a self-consistently determined effective medium scattering repeatedly from a given site [8]. It is exact for $d = \infty$ [9]. In the local approximation the self-energy is diagonal in the site representation and is therefore a function of energy only. The Falicov–Kimball model [10] in the homogeneous phase is mathematically equivalent to the Hubbard model with the alloy analogy approximation and the CPA therefore yields exact solutions of the Falicov–Kimball model for $d = \infty$ [11, 5].

The main defect of the alloy analogy approximation is that it never yields a normal Fermi liquid with a Migdal discontinuity and quasi-particle states of infinite lifetime at the Fermi surface [12]. This is because electrons of spin σ are scattering from disordered 'frozen' $-\sigma$ electrons; to obtain Fermi liquid behaviour it is essential to include the dynamics of the $-\sigma$ electrons [13, 1]. We now give a diagrammatic treatment of the self-energy which includes this dynamics and is exact within the local approximation. We use a site representation and follow as closely as possible the diagrammatic treatment of the alloy CPA [8]. Despite a formal similarity the meaning of the diagrams is different because there is no analogue of configurational averaging in the present many-body case. The diagrams for the proper self-energy $\Sigma = \Sigma_{ii}$ in the present local approximation are drawn in figure 1(*a*). The doubly-crosshatched parts of the diagrams are connected so that no diagram falls into two parts on cutting one of the double-line propagators and there are no self-energy insertions on any double line. The latter are included in the full propagator represented by the double line. However, non-nested diagrams such as that of figure 1(*b*) are included, which is a difference from the alloy CPA diagrams [8]. In fact figure 1(*a*) presents a complete set of self-energy diagrams; the only approximation is the local one in which each interaction of the propagating dressed electron with the rest of the system takes place at the same site i. The crosshatched parts of the diagrams, even if drawn as skeleton diagrams with self-energy insertions absorbed into full propagators everywhere, include interactions at sites other than i in general. However, in the special case $d = \infty$ interactions throughout a skeleton diagram may be restricted to site i [4]. In the following analysis we consider the self-energy Σ as a functional of the local propagator $G = G_{ii}$ represented by the double line. Thus we write $\Sigma = \Sigma[G]$ and in general we shall consider $\Sigma[\gamma]$ where γ is not restricted to be the true propagator G. However, all propagators in the rest of the diagram (the crosshatched region) are actual propagators appropriate to the model considered (e.g. Hubbard, Anderson impurity etc.).

Our first objective is to show how to derive the Hubbard alloy analogy

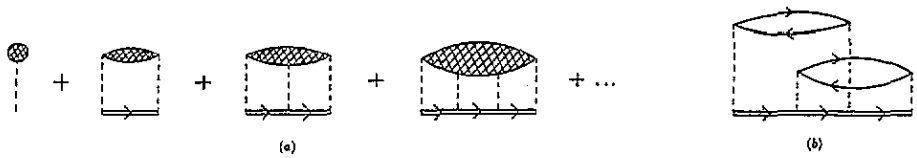

Figure 1. (*a*) A complete set of proper self-energy diagrams. All interactions of the double-line propagator occur at a single site i in the local approximation. (*b*) A non-nested diagram which is excluded from the related alloy CPA diagrams [8] but is included here.

diagrammatically and it is then straightforward to obtain the desired dynamical generalization. To do this we regroup the diagrams of figure 1(*a*) as shown in figure 2. The singly-crosshatched parts of the diagram in column 1 correspond to full n-particle Green functions

$$\langle T[n_{i-\sigma}(t_1)n_{i-\sigma}(t_2)\ldots n_{i-\sigma}(t_n)]\rangle \tag{2.2}$$

where T is the time-ordering operator. The singly-crosshatched regions therefore contain contributions from disconnected parts which must be subtracted, as shown in columns 2,3,.... Figure 2 is very similar to figure 11 of Elliott *et al* [8] although the meaning of the diagrams is rather different. The following analysis follows their work closely.

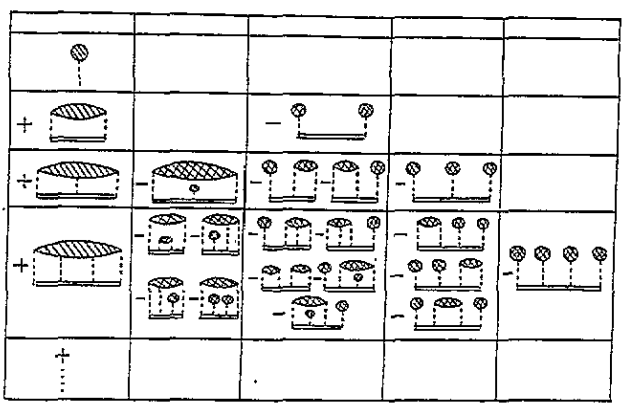

Figure 2. A regrouping of the diagrams of figure 1(*a*) as explained in the text.

We denote the sum of column 1 in figure 2 by $S[G]$, once again considering it as a functional of the double-line propagator. The sum of column 2 may be re-written as in figure 3 where the triple-line propagator is given by

$$\gamma = G + G\Sigma[\gamma]G + G\Sigma[\gamma]G\Sigma[\gamma]G + \ldots = G/(1-\Sigma[\gamma]G). \tag{2.3}$$

Thus the sum of column 2 is $-\Sigma[\gamma]+\Sigma[G]$, the sum of column 3 is $-\Sigma[\gamma]G\Sigma[\gamma]$ and so on. Hence, adding the column, we have

$$\Sigma[G] = S[G]+\Sigma[G]-\Sigma[\gamma]-\Sigma[\gamma]G\Sigma[\gamma]\ldots = S[G]+\Sigma[G]-\Sigma[\gamma]/(1-\Sigma[\gamma]G). \tag{2.4}$$

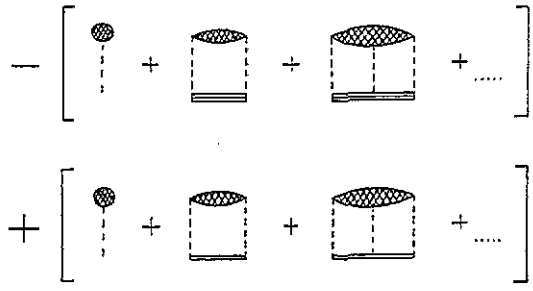

Figure 3. Another way of writing the sum of column 2 in figure 2, with triple-line propagator defined by equation (2.3).

Thus

$$\Sigma[\gamma] = S[G]/(1 + S[G]G). \tag{2.5}$$

Also, from equation (2.3),

$$G = \gamma/(1 + \gamma\Sigma[\gamma]) \tag{2.6}$$

which may be substituted in equation (2.5) to obtain an equation defining the functional $\Sigma[\gamma]$. Replacing γ by G in this equation we find the required self-energy $\Sigma = \Sigma[G]$ satisfies the equation

$$\Sigma = \frac{S[G/(1 + G\Sigma)]}{1 + S[G/(1 + G\Sigma)]G/(1 + G\Sigma)}. \tag{2.7}$$

This is an equation for Σ since for a given model the local Green function G is a known function of Σ. Thus for the Hubbard model

$$G = N^{-1}\sum_{k}(E - \epsilon_k - \Sigma)^{-1} = G^0(E - \Sigma) \tag{2.8}$$

where ϵ_k is the one-electron band energy and $G^0(E)$ is the one-electron Green function for the non-interacting system. Corresponding expressions for the Anderson lattice, d–p model and Anderson impurity may be written down immediately. For the Anderson impurity model the relationship between G and Σ is very simple and may be written as

$$G^{-1} = (G^0)^{-1} - \Sigma \tag{2.9}$$

where G^0 is the unperturbed Green function for the local orbital.

For equation (2.7) to be useful we need a way of calculating the functional $S[G]$. This is easy to do with the alloy analogy approximation. In this approximation the $-\sigma$ spin electrons are frozen, which corresponds to turning off $-\sigma$ spin hopping. Then $n_{i-\sigma}(t)$ is independent of time t and the Green function (2.2) is just $\langle n_{i-\sigma}\rangle$. In the absence of $-\sigma$ spin dynamics all the local propagators in column 1 of figure 2 are evaluated at the same energy and we can sum the terms in column 1 to obtain

$$S[G] = U\langle n_{-\sigma}\rangle(1 - UG)^{-1}. \tag{2.10}$$

Thus in the alloy analogy approximation $S[G]$ is a *function* of G; it is also *universal*, that is the same for all models. On substituting this form for S into equation (2.7) we easily obtain the standard CPA equation [8]

$$\Sigma = U\langle n_{-\sigma}\rangle/[1-(U-\Sigma)G] \tag{2.11}$$

for the self-energy of a σ-spin electron.

To go beyond the alloy analogy, and obtain a more useful form of equation (2.7) which is exact within the local approximation, it is convenient to introduce a new functional $S_1[G]$. This is defined as the sum of columns $1,3,4,5\ldots$ in figure 2, once again considered as a functional of the double-line propagator. The diagrams of column 2 are not subtracted so that the diagrams defining $S_1[G]$ take the form of the proper self-energy diagrams one would draw if the double line was a bare propagator, although all its interactions occur at site i. Thus $S_1[G^0]$ is the self-energy calculated with a restriction that the bare propagator at the base of each diagram has interactions at a single site i. Clearly

$$S[G] = S_1[G] + S_1[G]GS_1[G] + \ldots = S_1[G]/(1-GS_1[G]). \tag{2.12}$$

Using this relation in equation (2.7) we obtain

$$\Sigma = S_1[G/(1+G\Sigma)]. \tag{2.13}$$

This is the central result of this section and it requires some discussion.

Equation (2.13) states that within the local approximation we may calculate the self-energy exactly according to the following prescription: sum all self-energy diagrams, drawn with bare propagators, but with the propagator G^0 along the base of the diagram having interactions only at a single site i and being replaced by $G/(1+G\Sigma)$. The latter replacement compensates for the restriction to scattering at a single site. For the impurity model there *is* only one site and, from equation (2.9), $G/(1+G\Sigma) = G^0$. Hence the prescription just tells us to sum all self-energy diagrams so that for the impurity model equation (2.13) is a tautology. It follows from equations (2.12) and (2.10) that in the alloy analogy approximation $S_1[G]$ becomes

$$S_1^{\mathrm{AA}}[G] = U\langle n_{-\sigma}\rangle/[1-(1-\langle n_{-\sigma}\rangle UG] \tag{2.14}$$

a universal function of G. In general the functional $S_1[G]$ is model-dependent but in the case $d=\infty$ it becomes universal, for the following reason. Müller-Hartmann [4] pointed out that, for the Hubbard model in $d=\infty$, interactions in skeleton diagrams for Σ may be restricted to a single site. Hence Σ is a functional of the local Green function G and the functional is universal because the structure of the self-energy diagrams is identical for all models of the class considered. Clearly from equation (2.13), since Σ is a universal functional for G for $d=\infty$, S_1 is a universal functional in this limit. Thus, for $d=\infty$, S_1 may be determined for the simplest model, the Anderson impurity model, and is thus defined by

$$\Sigma_{\mathrm{imp}} = S_1[G^0_{\mathrm{imp}}]. \tag{2.15}$$

Hence S_1 is the functional relating the unperturbed local Green function and the self-energy for the impurity model. Equation (2.12) is then a useful equation to determine Σ exactly for any of the other models with $d=\infty$, provided one can calculate the self-energy for the impurity model with arbitrary unperturbed

propagator or, equivalently, arbitrary hybridization function $\Delta(E)$. This is the scheme recently proposed by several authors [5–7]. Methods used so far to calculate Σ_{imp} approximately include second-order perturbation theory [6] and Monte-Carlo methods [14–16]. Work in progress in our group makes use of numerical renormalization group methods developed here by Costi and Hewson [17]. All these methods are quite complicated numerically and so far do not yield clear-cut results on, for example, the transition between a Fermi liquid and non-Fermi liquid phase. The method of I yielded interesting results quite simply and the main purpose of the next section is to show that it can be fitted into the framework discussed in this section. This makes the striking results of I more plausible and in paper III of the series we shall give further details of the calculations reported rather briefly in I.

3. Earlier work from the new viewpoint

3.1. Kawabata's approach

We begin by showing how the early work of Kawabata [13] on the half-filled Hubbard band fits in to the general structure discussed in section 2. It turns out to be closely related to the second-order perturbation treatment of the $d = \infty$ limit used by Georges and Kotliar [6] and Zhang *et al* [18]. In this limit the equation determining the self-energy Σ may be written, according to equations (2.13) and (2.15), in the form

$$\Sigma = \Sigma_{\text{imp}}[G_0] \tag{3.1}$$

$$G_0^{-1} = G^{-1} + \Sigma. \tag{3.2}$$

Here the functional $\Sigma_{\text{imp}}[G_0]$ yields the self-energy of an Anderson impurity model with unperturbed Green function G_0. For the symmetric case of the Anderson model, corresponding to half filling in the Hubbard model, it is known that second-order perturbation theory is reasonable provided the expansion is made around the non-magnetic Hartree–Fock solution [19]; in particular it gives the correct atomic limit, with hybridization turned off, in the symmetric case. The unperturbed propagator is then the Hartree–Fock propagator given by

$$G_{\text{HF}}^{-1} = G_0^{-1} - Un \tag{3.3}$$

where $n = \langle n_{-\sigma} \rangle$ is the number of electrons per atom of one spin. The suffix σ is unecessary since we consider only paramagnetic states in this paper. The second-order contribution Σ_2 to $\Sigma_{\text{imp}}[G_0]$, corresponding to the simplest bubble diagram, is given by

$$\Sigma_2 = U^2 G_{\text{HF}}(t)^2 G_{\text{HF}}(-t) \tag{3.4}$$

or

$$\Sigma_2 = \mathrm{i}U^2 G_{\text{HF}}(t)\chi(t) \tag{3.5}$$

where $\chi(t) = -\mathrm{i}G_{\text{HF}}(t)G_{\text{HF}}(-t)$ is the non-interacting local-density response for electrons of one spin. Thus in the second-order treatment [6, 18] the self-energy is

given by $\Sigma = Un + \Sigma_2$ where Σ_2 satisfies equation (3.4) with the Fourier transform of $G_{HF}(t)$ replaced by a propagator whose inverse is

$$G^{-1} + \Sigma_2. \tag{3.6}$$

The last equation follows from equations (3.3) and (3.2). Kawabata [13] determined Σ_2 by using equation (3.5) and making the same replacement (3.6) for G_{HF} but introducing a phenomenological form for $\chi(t)$ corresponding to a full interacting response function. This procedure was motivated by comparison with the Hubbard alloy analogy. It is interesting that Zhang *et al* [18] find a metal–insulator transition for the half-filled Hubbard band whereas Kawabata [13] finds a metallic state for all finite U. To understand this difference we note that in an insulating state the Fermi level lies in the gap so that the imaginary parts of G and Σ_2 vanish at the Fermi energy. The imaginary part of the propagator replacing G_{HF}, whose inverse is expression (3.6), vanishes similarly and thus has a gap in its spectrum. In the strict second-order treatment of Zhang *et al* [18] the density response χ in (3.5) corresponds to a simple bubble of such propagators and hence corresponds to a non-interacting density fluctuation spectrum with a frequency gap. In Kawabata's treatment χ is a full density response for electrons of one spin; it is dominated by spin fluctuations at low frequency and quite generally $\mathrm{Im}\,\chi \propto \omega$ in both metallic and insulating states. It appears to be this which inhibits an insulating self-consistent solution based on equation (3.5). Clearly equation (3.5) is an unsatisfactory form for Σ_2, beyond the strict second-order treatment of equation (3.4), and a vertex correction would have to be introduced as done previously for the ferromagnetic Hubbard model [20] and high-field limit of the Anderson lattice [21]. Both equations (3.4) and (3.5) are unsatisfactory away from half filling of the band because they do not give the correct atomic limit.

3.2. The method of paper I

We first recall the method of paper I and then show how it may be regarded as adopting a type of functional S_1 in equation (2.13) which can give reasonable results for the test case of the Anderson impurity model.

In the Hubbard alloy analogy CPA approximation the second-order contribution to the self energy $\Sigma(E)$ of the Hubbard model is

$$U^2 n(1-n)G^0(E) \tag{3.7}$$

where G^0 is the Green function for the non-interacting system and n the number of electrons of each spin, as before. The correct second-order contribution in the local approximation may be written in the same form with $G^0(E)$ replaced by $\tilde{G}^0(E)$, the Fourier transform of

$$\tilde{G}^0(t) = \mathrm{i}G^0(t)\chi_0(t)/[n(1-n)] \tag{3.8}$$

where $\chi_0(t)$ is the non-interacting local density response for electrons of a given spin. It is convenient to use the corresponding retarded Green functions in the spectral representations

$$G^0(E) = \int \rho(\omega)(E-\omega)^{-1}\,\mathrm{d}\omega \tag{3.9}$$

$$\tilde{G}^0(E) = \int \tilde{\rho}(\omega)(E-\omega)^{-1}\,\mathrm{d}\omega \tag{3.10}$$

where $\rho(\omega)$ is the one-electron density of states for the non-interacting Hubbard band. $\tilde{\rho}(\omega)$ is a functional of $\rho(\omega)$ for given n and has the following important properties:

(i) if $\rho(\omega)$ is non-zero in the interval $(-W, W)$, $\tilde{\rho}(\omega)$ is non-zero in $(-3W, 3W)$;
(ii) the weight of $\tilde{\rho}(\omega)$ below and above E_F, the Fermi level in the band, is n and $1-n$, respectively, as for $\rho(\omega)$; and
(iii) $\tilde{\rho}(\omega) \simeq (\omega - E_F)^2$ near E_F.

The last property yields, to second-order, $\operatorname{Im}\Sigma(E) \propto \operatorname{Im}\tilde{G}^0(E) \propto (E-E_F)^2$ which ensures Fermi liquid behaviour. This is, of course, not the case for the Hubbard approximation (3.7).

We have pointed out that the correct second-order Σ in the local approximation may be obtained from the Hubbard alloy analogy result by replacing G^0 in (3.7) by a new unperturbed propagator $\tilde{G}^0$. The approximate procedure of I is to make this replacement to all orders so that the CPA equation (2.11) for $\Sigma(E)$, in which $G = \tilde{G}^0(E-\Sigma)$ from equation (2.8), becomes

$$\Sigma = Un[1-(U-\Sigma)\tilde{G}^0(E-\Sigma)]^{-1}. \tag{3.11}$$

In the calculations of I we used the semi-elliptic band

$$\rho(E) = (2/\pi W)[1-(E/W)^2]^{1/2} \tag{3.12}$$

and approximated the corresponding $\tilde{\rho}(E)$ by a reasonable and convenient analytic expression having the three properties described above. We shall discuss the half-filled band case ($E_F = 0$) in detail where we took

$$\tilde{\rho}(E) = (E/c)^2\rho(E/c)/[a^2 + b^2(E/c)^2] \tag{3.13}$$

usually assuming $b = 0$. The parameter c is a scale factor ($\simeq$ 2–3) which allows for property (i) of $\tilde{\rho}$ and the E^2 factor ensures property (iii). The parameters a, b and c are related by the normalization condition $\int \tilde{\rho}(E)\,\mathrm{d}E = 1$.

Equations (3.13), (3.10) and (3.11) define the scheme used in I to calculate the self-energy Σ of a Hubbard model with unperturbed density of states $\rho(E)$. Equation (3.11) may be regarded as derived from the general equation (2.12) with the following definition of the functional S_1:

$$S_1[G/(1+G\Sigma)] = S_1^{AA}[\tilde{G}/(1+\tilde{G}\Sigma)] \tag{3.14}$$

where, for $G = \tilde{G}^0(E-\Sigma)$, $\tilde{G} = \tilde{G}^0(E-\Sigma)$ and S_1^{AA} is defined by equation (2.14). Clearly $S_1(g)$, as defined, is not a universal functional of g. Its evaluation involves first writing g in the form $g = G/(1+G\Sigma)$, where Σ is the self-energy (to be determined) of the particular model, and then replacing G by $\tilde{G}$ in a prescribed manner. It was pointed out in section 2 that in general the exact functional S_1 is not universal.

Clearly the above definition of S_1, leading to equation (3.11) for Σ as used in I, is somewhat arbitrary. Its main justification is a correct atomic limit and a qualitatively correct small-U limit. We now apply it to the test case of the symmetric Anderson impurity model and show that it can give certain essential results correctly. For the standard impurity model $\rho(E)$ is the Lorentzian function

$$\rho(E) = \pi^{-1}\Delta/(E^2+\Delta^2). \tag{3.15}$$

Hence, from equations (3.13) and (3.15),

$$\tilde{\rho}(E) = (1/c\pi)[\Delta/(x^2 + \Delta^2)][(1-\beta)x^2/(\beta^2\Delta^2 + (1-\beta)^2x^2)] \tag{3.16}$$

with $x = E/c$. The parameters a and b in equation (3.13) have been replaced by a single parameter β, defined by $(1-\beta)/\beta = b\Delta/a$, so that $\tilde{\rho}(E)$ is correctly normalized. The corresponding Green function given by equation (3.10) is

$$\tilde{G}^0(E) = [(1-\beta)/c][(x^2(x + i\Delta)^{-1} - \beta x)/(\beta^2\Delta^2 + (1-\beta)^2x^2)]. \tag{3.17}$$

Equations (3.11) and (3.17) define Σ and an expansion of equation (3.11) around the Fermi level, given by $\mu = U/2$ in the symmetric case considered, yields the renormalization factor

$$z = (1 - d\Sigma/dE)^{-1}_{E=\mu} = 1 - (u^2/4c)[(1-\beta)/\beta] \tag{3.18}$$

where $u = U/\Delta$. For the impurity model considered here z should be positive for all U, ensuring Fermi liquid behaviour, and its value determines the width of the Kondo resonance in the one-electron spectrum at the Fermi level. For correct Kondo behaviour $z \sim \exp(-\pi U/8\Delta)$ for $U \gtrsim \Delta$ and this can be simulated by the following choice of the principal parameter appearing in our functional:

$$b\Delta/a = (1-\beta)/\beta = (4c/u^2)[1 - \exp(-\pi u/8)]. \tag{3.19}$$

This choice ensures the correct width of the Kondo resonance for all U; its height is correctly given by the height $(\pi\Delta)^{-1}$ of the resonance in the non-interacting case $U = 0$ since $G = G^0(E - \Sigma)$, and $E = \Sigma = U/2$ at the Fermi level $E = \mu$, so that $\mathrm{Im}\, G(\mu) = \mathrm{Im}\, G^0(0)$. Furthermore the correctness of the atomic limit ensures that the other two peaks in the spectrum occur about $E = \pm U/2$ as they should. The non-zero value of b is essential for the Lorentzian $\rho(E)$, otherwise $\tilde{\rho}(E)$, given by equation (3.13), does not tend to zero as $E \to \pm\infty$. For Hubbard models with finite bandwidth a non-zero b does not play a crucial role and at half filling Fermi liquid theory breaks down for U greater than a critical value, as shown in I, whether b is zero or non-zero. The critical U depends on the value of b but taking $b = 0$ does not make any qualitative change.

4. Discussion

An important class of model Hamiltonians with on-site electron interaction includes the Hubbard model, d–p model, periodic Anderson model and the Anderson impurity model. An exact diagrammatic analysis of the electron self-energy Σ of such models is given in section 2 within the local approximation. It is shown that Σ satisfies an equation involving a functional which is in general model-dependent. However, for dimension $d = \infty$, where the local approximation is exact [3, 4], the functional is universal and may be evaluated using an auxiliary impurity model. The latter scheme was recently developed by several authors [5–7] with starting-points different from the present one. In section 3 it is shown that the earlier approach of paper I of this series may be fitted into the new framework and can lead to sensible results for the test case of the Anderson impurity model. This lends more weight to results of I and further details of this work will be given in paper III of the series. The advantage of this approximate method is that Σ satisfies an explicit algebraic or transcendental

equation so that many results can be obtained analytically, and it is essentially correct in the weak-coupling and atomic limits for arbitrary electron density. The most striking result of I is that for paramagnetic solutions of the Hubbard model Fermi liquid behaviour breaks down in a whole region of the $T = 0$ phase diagram, not just on the insulating part of the line corresponding to a half-filled band as found by Brinkman and Rice [22]. It is of the highest interest to test this prediction using the new more rigorous methods which are exact for $d = \infty$. Most work so far along these lines is restricted to the half-filled band case [6, 14–16]. The main problem is to solve the auxiliary impurity model and methods used so far have their limitations. Second-order perturbation theory [6] is unreliable away from half filling, because it does not give the atomic limit correctly, and with Monte Carlo methods [14–16] it is difficult to approach $T = 0$ where the interesting phase transition occurs. Numerical renormalization group methods being developed in our group are promising.

References

[1] Edwards D M and Hertz J A 1990 *Physica* B **163** 527
[2] Hubbard J 1964 *Proc. R. Soc.* A **281** 401
[3] Metzner W and Vollhardt D 1989 *Phys. Rev. Lett.* **62** 324
[4] Müller-Hartmann E 1989 *Z. Phys.* B **74** 507
[5] Janis V 1991 *Z. Phys.* B **83** 227
[6] Georges A and Kotliar G 1992 *Phys. Rev.* B **45** 6479
[7] Janis V and Vollhardt D 1992 *Int. J. Mod. Phys.* B **6** 731
[8] Elliott R J, Krumhansl J A and Leath P L 1974 *Rev. Mod. Phys.* **46** 465
[9] Schwartz L and Siggia E 1972 *Phys. Rev.* B **5** 383
Vlaming R and Vollhardt D 1992 *Phys. Rev.* B **45** 4637
[10] Falicov L M and Kimball J C 1969 *Phys. Rev. Lett.* **22** 997
[11] Brandt U and Mielsch C 1989 *Z. Phys.* B **75** 365; 1990 *Z. Phys.* B **79** 295; 1991 *Z. Phys.* B **82** 37
[12] Edwards D M and Hewson A C 1968 *Rev. Mod. Phys.* **40** 810
[13] Kawabata A 1975 *Prog. Theor. Phys.* **54** 45
[14] Georges A and Krauth W 1992 *Phys. Rev. Lett.* **69** 1240
[15] Rozenberg M J, Zhang X Y and Kotliar G 1992 *Phys. Rev. Lett.* **69** 1236
[16] Jarrel M 1992 *Phys. Rev. Lett.* **69** 168
[17] Costi T A and Hewson A C 1992 *Phil. Mag.* B **6** 1165
[18] Zhang X Y, Rozenberg M J and Kotliar G *Preprint* Rutgers University, USA
[19] Yamada K 1975 *Prog. Theor. Phys.* **53** 970
Horvatić B and Zlatić V 1980 *Phys. Status Solidi* b **99** 251
[20] Hertz J A and Edwards D M 1973 *J. Phys. F: Met. Phys.* **3** 2174
Edwards D M and Hertz J A 1973 *J. Phys. F: Met. Phys.* **3** 2191
[21] Edwards D M 1991 *Physica* B **169** 271
[22] Brinkman W F and Rice T M 1970 *Phys. Rev.* B **2** 4302